Chemodivergent Organolanthanide Catalyzed C-H α-Mono-Borylation of Azines

Jacob O. Rothbaum,[1] Alessandro Motta,[2*] Yosi Kratish,[1*] and Tobin J. Marks[1*]

[1]Department of Chemistry, Northwestern University, Evanston, Illinois 60208-3113, United States

[2]Dipartimento di Scienze Chimiche, Università di Roma "La Sapienza" and INSTM, UdR Roma, Piazzale Aldo Moro 5, I-00185 Roma, Italy

*e-mail: alessandro.motta@uniroma1.it, yosi.kratish@northwestern.edu, t-marks@northwestern.edu

C-H activation and functionalization of pyridinoid azines is a key transformation for the synthesis of many natural products, pharmaceuticals, and materials. Reflecting the azinyl nitrogen lone-pair steric repulsion, tendency to irreversibly bind to metal ion catalysts, and the electron-deficient nature of pyridine, C-H functionalization at the important α-position remains challenging. Thus, the development of earth-abundant catalysts for the α-selective mono-functionalization of azines is a crucial hurdle for modern chemical synthesis. Here, the selective organolanthanide-catalyzed α-mono-borylation of a diverse series of pyridines is reported, affording a valuable precursor for cross-coupling reactions. Experimental and theoretical mechanistic evidence support the formation of a C-H activated η^2-lanthanide-azine complex, followed by intermolecular α-mono-borylation via σ-bond metathesis. Notably, varying the lanthanide identity and substrate electronics promotes chemodivergence of the catalytic selectivity: smaller/more electrophilic lanthanide^{3+} ions and electron-rich substrates favor selective α-C-H

functionalization, whereas larger/less electrophilic lanthanide^{3+} ions and electron-poor substrates favor selective B-N bond-forming 1,2-dearomatization. Such organolanthanide series catalytic chemodivergence is, to our knowledge, unprecedented.

Developing new catalytic routes to C-H functionalized molecules with high regio- and chemoselectivity for the efficient generation of high-value products is an ongoing "grand challenge" in chemical science, owing both to the ubiquity and relative inertness of molecular C-H bonds.[1] A catalyst that can selectively functionalize these moieties in fewer steps would accelerate the creation of numerous complex molecules and materials. Moreover, if such catalysts could be easily and rationally altered to afford chemodivergent reactivity patterns, it would be an even more valuable tool for imparting structural diversity.[2] Regarding specific target families, pyridines are pervasive as ligands and directing groups, ubiquitous moieties in pharmaceuticals and natural products, and are the second most common aromatics in pharmaceuticals, with monosubstituted pyridines having functionality at the difficultly accessed α-position predominant.[3] Therefore, developing more efficient and selective ways of functionalizing pyridines would be important for advancing synthetic methodology towards essential compounds.

Currently, the principal methods of functionalizing pyridine and related azines are via *N*-activated azines, deprotonative metalation, S_nAr, radical, and transition metal-based catalysis.[4,5] Despite significant advances, many of these useful reactions require activated substrates or cannot achieve high selectivity without steric-blocking or directing

groups.[6-8] Note that powerful heteroaromatic functionalization reactions such as Minisci- and Chichibabin-type radical substitutions utilize precious metals, in catalytic and/or stoichiometric amounts, and often require electron-poor substrates.[9-12] There have been impressive strides in the C-H functionalizations of pyridine, specifically the α-position; however, a major drawback is the necessity to substitute and/or block the other skeletal positions to prevent catalyst poisoning and/or improve regioselectivity, which limits the potential impact (Fig. 1a).[13-15] These obstacles highlight the need to develop catalytic processes which selectively functionalize various positions on pyridine-related substrates with earth-abundant metals.[16]

In regard to modifying pyridinoids, many prominent synthetic precursors/intermediates utilize reactive boron moieties (e.g., -Bpin) which, once introduced, can be readily exchanged for diverse target functional groups in transformations such as Suzuki-Miyuara cross-coupling.[17] These precursors have been shown to be essential for the late-stage functionalization of many natural products and pharmaceuticals,[18,19] and are useful for cross-coupling reactions.[20-25] Pyridine borylation at the β– and γ–positions can now be achieved with efficiency, [26-30] but C-H borylation of the α-position remains challenging.[31] This reflects the inherent electron deficiency of pyridines which depresses reactivity, the susceptibility of C-H α-borylated products to rapid protodeboronation over a range of pHs, the nitrogen lone pair steric impediment, and irreversible binding to many catalytic metal centers.[32,33] In contrast, the high coordination numbers, kinetic lability, and very polar metal-ligand bonding of electrophilic lanthanide-organic complexes have proven effective in diverse heteroatom hydroelementation and polymerization processes.[34] These

characteristics and the evidence that lanthanide catalysts frequently operate by entirely different reaction mechanisms than d-block catalysts[35] raise the intriguing question of whether they might activate pyridines via unusual and potentially useful reactivity modalities.

To date, the only documented organolanthanide-mediated α-pyridine activation has come at the expense of restrictive blocking groups and/or additives to assist turnover (Fig. 1a).[36-39] This Laboratory recently reported highly 1,2 -selective B-N bond-forming pyridine dearomatization using an organolanthanum (La) catalyst with high atom-efficiency (Fig. 1b).[40] Considering the large, multiple ligands accommodating La^{3+} (ionic radius = 1.250 Å), we hypothesized that a smaller lanthanide such as Lu^{3+} (ionic radius = 0.995 Å) with demonstrated C-H activation capacity,[41,42] might force pyridine activation along with an alternative and useful pathway. Here we report the organolanthanide-catalyzed α-mono-borylation of a diverse series of pyridines (Fig. 1b) using medium to small ionic radii (1.175→0.995 Å) organolanthanide catalysts. It will be seen that this process is regio- and chemo-selective and can tolerate a variety of functional groups. To elucidate the fundamental origin of the selectivity of these catalysts, we report detailed kinetic/mechanistic studies supported by solid-state structures and DFT computation. In clarifying the reaction mechanism, we reveal what is, to our knowledge, the first example of chemodivergent reactivity within lanthanide catalytic science.

The present organolanthanide-catalyzed C-H functionalization of pyridines with pinacolborane (HBpin) was examined under anhydrous/anaerobic conditions using a

series of $Cp^*_2LnCH(TMS)_2$ precatalysts where Ln = La, Nd, Sm, Lu, and Y. The reaction conditions are mild and straightforward (see Supporting Information for experimental details). Strikingly, while surveying the lanthanide series, contracting the Ln^{3+} size was found to incrementally shift the selectivity as shown in Figure 2c: La^{3+} selectively produces 1,2-dearomatization, Nd^{3+} affords equal amounts of dearomatized and borylated product, Sm^{3+} primarily creates the borylated product and, finally, Y^{3+} and Lu^{3+} effect exclusive α-C-H borylation. Lu was selected going forward and, with optimized conditions in hand, substituent effects and mechanism were next examined. Figure 2a summarizes results for a series of variously substituted pyridines, substituent effects, catalyst:substrate ratio, and reaction temperature, revealing that selective α-mono-borylation is readily achieved with a 1:1 pyridine:HBpin ratio and 1-6 mol% $Cp^*_2LuCH(TMS)_2$ precatalyst at 80˚C-100˚C in toluene solution. Products were characterized by ^1H, ^{11}B, ^{13}C NMR spectroscopy, high-resolution mass spectrometry (HRMS), and in some cases, X-ray crystallography.

Within this pyridine series, both steric and electronic factors significantly influence reaction rates (Fig. 2a). Thus, dimethylaminopyridine (DMAP) undergoes borylation using 1 mol% catalyst loading yielding the borylated product **4a** exclusively in the form of a dimer, which was confirmed by NMR, HRMS, and X-ray crystallography (Fig. 2b). Similarly, several more heterocyclic Lewis base-substituted pyridines undergo borylation in high yields, with rapid rates, without the need for protecting groups yielding the corresponding borylated products, **4b, 4c, 4d**, and afford negligible 1,2-dearomatization side product. The structure of **4d** was also confirmed by X-ray crystallography (Fig. 2b). Note that the N-H moiety of a secondary amine substituent is well-tolerated without

protection, affording **4e** in good yield. Pyridines with other oxygen-containing substituents afford borylated products **4f** and **4g** in satisfactory yields despite the oxophilic nature of lanthanides. Pyridine and various alkylated pyridines generate mono-functionalized products **4h** - **4m** in acceptable yields and with negligible functional group borylation. Electron-deficient functional groups such as 4,4'-bipyridine (**4n**) and 4-CF_3 (**4o**) are tolerated and produce the borylated product. In all cases, when both pyridine α-positions are vacant, only monoborylation products are observed. While electroneutral/donating substituents at the γ-position are effective, electron-withdrawing and bulky groups suppress activity for reasons which are discussed in the theory section below.

Detailed ^{1}H NMR spectroscopic kinetic studies (Fig. S1) indicate a rate law which is first-order in Lu concentration, half-order in pyridine concentration, and inverse half-order in HBpin concentration (eq. 1). Here NMR reveals a DMAP-HBpin adduct formation,[43] which is confirmed by X-ray crystallography, and suggests that HBpin acts as an inhibitor,[44] competing with pyridine in binding to the electrophilic Lu center. The C-H activation of pyridine proceeds with an experimental KIE of 2.8 ± 0.2, and variable-temperature kinetic measurements and standard Eyring kinetic analyses yield activation parameters $\Delta H^{\neq}$ = 13.0(0.2) kcal mol^{-1}, $\Delta S^{\neq}$ = -41.1(0.7) cal mol^{-1}, and E_a = 13.7(0.2) kcal mol^{-1} (Fig. S3), in good agreement with theory (*vide infra*). The large negative $\Delta S^{\neq}$ implies a highly organized transition state which is a hallmark of many d^0, f^n – centered catalytic processes involving Lewis basic heteroatom substrates.[40] Additional DFT mechanistic analysis is presented below.

$$rate = \frac{k[Lu]^1[DMAP]^{1/2}}{[HBpin]^{1/2}} \quad (1)$$

To further probe the reaction mechanism, DFT calculations were undertaken to quantitatively investigate the C-H borylation pathway using DMAP (**4a**) as a model substrate (Figs. 3 and 4a). In the first step, DMAP coordinates to the $Cp^*_2LuCH(TMS)_2$ precatalyst, which is slightly exergonic (ΔG = -0.9 kcal mol^{-1}) (Fig. 3). Here and beyond, the half-order likely reflects a dissociative equilibration of the azine-HBpin adduct to the reactive precursors, which by DFT is slightly endergonic and strongly exothermic (ΔG_{dissoc} = 2.3 kcal mol^{-1}, ΔH = -9.4 kcal mol^{-1}) (Fig. 3).[44] Next, a concerted 4-center σ-bond metathesis H transfer from the DMAP α-position cleaves the Lu-$CH(TMS)_2$ bond to yield η^2-complex **III**, which is structurally confirmed by NMR and X-ray crystallography (Fig. 3), in a highly exergonic ΔG = -20.5 kcal mol^{-1} step with a barrier of $\Delta G^{\ddagger}$ = 28.5 kcal mol^{-1} (**TS1**) (see SI). Note that a stoichiometric $Cp^*_2LuCH(TMS)_2$ + DMAP 6h/80˚C reaction quantitatively yields complex **III**, supporting the proposed step. Once complex **III** is formed, HBpin associates and undergoes σ-bond metathesis, forming a new B-C bond at the DMAP α-position (**IV**). This step is computed to be exergonic by -11.9 kcal mol^{-1} with a barrier of $\Delta G^{\ddagger}$ = 12.1 kcal mol^{-1} (**TS2**) to yield the lowest energy intermediate on the reaction coordinate and is the TOF-determining intermediate (**TDI**).[45] Similar structures have been reported before and are likely stabilized in part by the μ_2-M-H-B bonding.[46] Next an equilibrium is established between complexes **IV** and **V** with an additional DMAP coordinating to the catalytic center (ΔG = 3.3 kcal mol^{-1}). This triggers the slightly endergonic (ΔG = 4.6 kcal mol^{-1}) release of the C-H borylated product from **V** via H^- transfer to the Lu center, yielding intermediate **VI**. From there the catalytic transformation is driven by product dimerization that is both exothermic and exergonic, ΔH = -30.3 kcal

mol^{-1}; ΔG = -8.4 kcal mol^{-1}, respectively, affording complex (**VI**). Note that the greater DMAP electron density within the borylated product is favored more than the corresponding pyridine dimer by $\Delta\Delta$H = -6.6 kcal mol^{-1} and $\Delta\Delta$G = -5.0 kcal mol^{-1} and the corresponding 4-(trifluoromethyl)pyridine dimer by $\Delta\Delta$H = -9.1 kcal mol^{-1} and $\Delta\Delta$G = -6.7 kcal mol^{-1}, consistent with the yield trends in Figures 2a and S80. From Figure 3, note that complex **VI** undergoes H_2 elimination, detectable by ^{1}H NMR, to restore **III** for a new cycle. This step is slightly exergonic with a barrier of $\Delta G^{\ddagger}$ = 24.5 kcal mol^{-1} (**TS3**) and is the TOF-determining transition state (TDTS)[45] with a calculated KIE of 2.8, in good agreement with the experimental KIE of 2.8 ± 0.2. Separately, the hydride analogue [Cp$_2$*LuH]$_2$ was surveyed and found to catalyze similar reactivity patterns, further supporting this mechanism. The overall energetic span is 28.2 kcal mol^{-1} when considering **IV** as the TDI species and **TS3** as the TDTS species.

The origin of the intriguing selectivity sensitivity to Ln identity was next analyzed by DFT, noting that C-H functionalization and 1,2-dearomatization share a common entry point (**I** in Fig. 4a). It is found that Lu has the greatest barrier for the 1,2 -dearomatization, $\Delta G^{\ddagger}$ = 33.4 kcal mol^{-1}, which is 1.6 kcal mol^{-1} greater than La (Fig. S81) and in good agreement with the experiment. Furthermore, $\Delta\Delta G^{\ddagger}_{\text{1,2dearo-CHboryl}}$ = +5.2 and -4.5 kcal mol^{-1} for Lu and La, respectively, again in agreement with experiment (Fig. 2c). It is likely that ligand-ligand and ligand-substrate non-bonded repulsions play a significant role as the Ln^{3+} ionic radius contracts from La^{3+} (1.250 Å) to Lu^{3+} (0.995 Å). Note that the 1,2–dearomatization pathway (Fig. 4a, left) requires binding of a second pyridine molecule which should be less favorable as the ligand sphere contracts. This is also supported by the crystal

structures of the complexes and the sterics quantified in free volume maps[47] (Figs. 4b and c). C-H borylation may also be promoted by the more electrophilic Lu^{3+} and less hydridic hydride (Table S12). Additionally, DFT examination of the chemodivergence in substituent effects (Table S13) reveals that $\Delta\Delta G^{\ddagger}_{1,2dearo\text{-}CHboryl}$ falls from the most electron-rich substrate, DMAP (+5.2 kcal mol^{-1}), to pyridine, (+2.6 kcal mol^{-1}), and to 4-(trifluoromethyl)pyridine (+0.3 kcal mol^{-1}). Moreover, substituent π–donation creates a more electron-rich azine which stabilizes dimers (Fig. S80). Finally, electron-poor pyridines should be susceptible to α-position nucleophilic attack by Ln-H moieties, in view of their close proximity (**I** in Fig. 4a), yielding 1,2 – dearomatized product.

In conclusion we report marked chemodivergence in an organolanathanide-mediated catalytic reaction involving a broad class of pyridinoid substrates: the crossover with lanthanide identity from highly selective HBpin-delivering B-N bond-forming dearomatization to highly α-C-H functionalization/borylation with HBpin. Regarding the latter pathway, experimental and theoretical mechanistic data support the formation of a C-H activated η^2-lanthanide-azine complex, followed by intermolecular α-mono-borylation via σ-bond metathesis. Varying the lanthanide identity and substrate electronics promotes chemodivergence of the catalytic selectivity: smaller/more electrophilic $lanthide^{3+}$ ions and electron-rich substrates favor selective α-C-H functionalization, whereas larger/less electrophilic $lanthanide^{3+}$ ions and electron-poor substrates favor selective B-N bond-forming 1,2-dearomatization. Such organolanthanide series catalytic chemodivergence is, to our knowledge, unprecedented and relevant to the placement of early lanthanides in the Periodic Table.[48,49]

References

1 Campos, K. R. *et al.* The importance of synthetic chemistry in the pharmaceutical industry. *Science* **363**, (2019).

2 Beletskaya, I. P., Nájera, C. & Yus, M. Chemodivergent reactions. *Chem. Soc. Rev.* **49**, 7101-7166, (2020).

3 Vitaku, E., Smith, D. T. & Njardarson, J. T. Analysis of the Structural Diversity, Substitution Patterns, and Frequency of Nitrogen Heterocycles among U.S. FDA Approved Pharmaceuticals. *J. Med. Chem.* **57**, 10257-10274, (2014).

4 Zhang, X. *et al.* Phosphorus-mediated sp2–sp3 couplings for C–H fluoroalkylation of azines. *Nature* **594**, 217-222, (2021).

5 Li, Z. *et al.* A tautomeric ligand enables directed C–H hydroxylation with molecular oxygen. *Science* **372**, 1452, (2021).

6 Campeau, L.-C., Rousseaux, S. & Fagnou, K. A Solution to the 2-Pyridyl Organometallic Cross-Coupling Problem: Regioselective Catalytic Direct Arylation of Pyridine N-Oxides. *J. Am. Chem. Soc* **127**, 18020-18021, (2005).

7 O'Hara, F., Blackmond, D. G. & Baran, P. S. Radical-Based Regioselective C–H Functionalization of Electron-Deficient Heteroarenes: Scope, Tunability, and Predictability. *J. Am. Chem. Soc.* **135**, 12122-12134, (2013).

8 Murakami, K., Yamada, S., Kaneda, T. & Itami, K. C-H functionalization of azines. *Chem. Rev.* **117**, 9302-9332, (2017).

9 Fujiwara, Y. *et al.* Practical and innate carbon–hydrogen functionalization of heterocycles. *Nature* **492**, 95-99, (2012).

10 Fier, P. S. & Hartwig, J. F. Selective C-H Fluorination of Pyridines and Diazines Inspired by a Classic Amination Reaction. *Science* **342**, 956, (2013).

11 Jin, J. & MacMillan, D. W. C. Alcohols as alkylating agents in heteroarene C–H functionalization. *Nature* **525**, 87-90, (2015).

12 Kim, J. H. *et al.* A radical approach for the selective C–H borylation of azines. *Nature* **595**, 677-683, (2021).

13 Oeschger, R. J., Larsen, M. A., Bismuto, A. & Hartwig, J. F. Origin of the Difference in Reactivity between Ir Catalysts for the Borylation of C–H Bonds. *J. Am. Chem. Soc.* **141**, 16479-16485, (2019).

14 Sadler, S. A. *et al.* Iridium-catalyzed C–H borylation of pyridines. *Org. Biomol. Chem.* **12**, 7318-7327, (2014).

15 Obligacion, J. V., Semproni, S. P. & Chirik, P. J. Cobalt-catalyzed C-H borylation. *J. Am. Chem. Soc.* **136**, 4133-4136, (2014).

16 Nuss, P. & Eckelman, M. J. Life Cycle Assessment of Metals: A Scientific Synthesis. *PLOS ONE* **9**, e101298, (2014).

17 Boström, J., Brown, D. G., Young, R. J. & Keserü, G. M. Expanding the medicinal chemistry synthetic toolbox. *Nat. Rev. Drug Disc.* **17**, 709-727, (2018).

18 Guillemard, L., Kaplaneris, N., Ackermann, L. & Johansson, M. J. Late-stage C–H functionalization offers new opportunities in drug discovery. *Nat. Rev. Chem.* **5**, 522-545, (2021).

19 Newton, J. N., Fischer, D. F. & Sarpong, R. Synthetic Studies on Pseudo-Dimeric Lycopodium Alkaloids: Total Synthesis of Complanadine B. *Angew. Chem. Int. Ed.* **52**, 1726-1730, (2013).

20 Malapit, C. A., Bour, J. R., Brigham, C. E. & Sanford, M. S. Base-free nickel-catalysed decarbonylative Suzuki–Miyaura coupling of acid fluorides. *Nature* **563**, 100-104, (2018).
21 Guo, P. *et al.* Micelle-Enabled Suzuki–Miyaura Cross-Coupling of Heteroaryl Boronate Esters. *J. Org. Chem.* **83**, 7523=7527 (2018).
22 Yang, D. X. *et al.* Palladium-Catalyzed Suzuki−Miyaura Coupling of Pyridyl-2-boronic Esters with Aryl Halides Using Highly Active and Air-Stable Phosphine Chloride and Oxide Ligands. *Org. Let.* **11**, 381-384, (2009).
23 Deng, J. Z. *et al.* Copper-facilitated Suzuki reactions: application to 2-heterocyclic boronates. *Org. Let.* **11**, 345-347, (2009).
24 Billingsley, K. L. & Buchwald, S. L. A General and Efficient Method for the Suzuki–Miyaura Coupling of 2-Pyridyl Nucleophiles. *Angew. Chem. Int. Ed.* **47**, 4695-4698, (2008).
25 Mkhalid Ibraheem, A. I. *et al.* Ir-Catalyzed Borylation of C-H Bonds in N-Containing Heterocycles: Regioselectivity in the Synthesis of Heteroaryl Boronate Esters. *Angew. Chem. Int. Ed.* **45**, 489-491, (2006).
26 Trouvé, J., Zardi, P., Al-Shehimy, S., Roisnel, T. & Gramage-Doria, R. Enzyme-like Supramolecular Iridium Catalysis Enabling C−H Bond Borylation of Pyridines with meta-Selectivity. *Angew. Chem. Int. Ed.* **60**, 18006-18013, (2021).
27 Kuninobu, Y., Ida, H., Nishi, M. & Kanai, M. A meta-selective C–H borylation directed by a secondary interaction between ligand and substrate. *Nat. Chem.* **7**, 712-717, (2015).
28 Yang, L., Uemura, N. & Nakao, Y. meta-Selective C–H Borylation of Benzamides and Pyridines by an Iridium–Lewis Acid Bifunctional Catalyst. *J. Am. Chem. Soc.* **141**, 7972-7979, (2019).
29 Bisht, R., Hoque, M. E. & Chattopadhyay, B. Amide Effects in C−H Activation: Noncovalent Interactions with L-Shaped Ligand for meta Borylation of Aromatic Amides. *Angew. Chem. Int. Ed.* **57**, 15762-15766, (2018).
30 Davis, H. J., Mihai, M. T. & Phipps, R. J. Ion Pair-Directed Regiocontrol in Transition-Metal Catalysis: A Meta-Selective C–H Borylation of Aromatic Quaternary Ammonium Salts. *J. Am. Chem. Soc.* **138**, 12759-12762, (2016).
31 Larsen, M. A. & Hartwig, J. F. Iridium-catalyzed C–H borylation of heteroarenes: scope, regioselectivity, application to late-stage functionalization, and mechanism. *J. Am. Chem. Soc.* **136**, 4287-4299, (2014).
32 Cook, X. A. F., de Gombert, A., McKnight, J., Pantaine, L. R. E. & Willis, M. C. The 2-Pyridyl Problem: Challenging Nucleophiles in Cross-Coupling Arylations. *Angew. Chem. Int. Ed.* **60**, 11068-11091, (2021).
33 Cox, P. A. *et al.* Base-Catalyzed Aryl-B(OH)2 Protodeboronation Revisited: From Concerted Proton Transfer to Liberation of a Transient Aryl Anion. *J. Am. Chem. Soc.* **139**, 13156-13165, (2017).
34 Farnaby, J. H., Chowdhury, T., Horsewill, S. J., Wilson, B. & Jaroschik, F. Lanthanides and actinides: Annual survey of their organometallic chemistry covering the year 2019. *Coord. Chem. Rev.* **437**, 213830, (2021).
35 Arnold, P. L., McMullon, M. W., Rieb, J. & Kuhn, F. E. C-H bond activation by f-block complexes. *Angew. Chem. Int. Ed.* **54**, 82-100, (2015).

36 Kundu, A., Inoue, M., Nagae, H., Tsurugi, H. & Mashima, K. Direct ortho-C–H Aminoalkylation of 2-Substituted Pyridine Derivatives Catalyzed by Yttrium Complexes with N,N′-Diarylethylenediamido Ligands. *J. Am. Chem. Soc.* **140**, 7332-7342, (2018).
37 Song, G., Wang, B., Nishiura, M. & Hou, Z. Catalytic C-H bond addition of pyridines to allenes by a rare-Earth catalyst. *Chem. Eur. J.* **21**, 8394-8398, (2015).
38 Nagae, H., Shibata, Y., Tsurugi, H. & Mashima, K. Aminomethylation reaction of ortho-pyridyl C-H bonds catalyzed by group 3 metal triamido complexes. *J. Am. Chem. Soc.* **137**, 640-643, (2015).
39 Song, G., O, W. W. & Hou, Z. Enantioselective C-H bond addition of pyridines to alkenes catalyzed by chiral half-sandwich rare-earth complexes. *J. Am. Chem. Soc.* **136**, 12209-12212, (2014).
40 Dudnik, A. S., Weidner, V. L., Motta, A., Delferro, M. & Marks, T. J. Atom-efficient regioselective 1,2-dearomatization of functionalized pyridines by an earth-abundant organolanthanide catalyst. *Nat. Chem.* **6**, 1100-1107, (2014).
41 Watson, P. L. Facile C–H activation by lutetium–methyl and lutetium–hydride complexes. *J. Chem. Soc. Chem. Commun.*, 276-277, (1983).
42 D'Angelo, P. *et al.* Revised Ionic Radii of Lanthanoid(III) Ions in Aqueous Solution. *Inorg. Chem.* **50**, 4572-4579, (2011).
43 McLellan, R., Kennedy, A. R., Mulvey, R. E., Orr, S. A. & Robertson, S. D. 1-Alkali-metal-2-alkyl-1,2-dihydropyridines: Soluble Hydride Surrogates for Catalytic Dehydrogenative Coupling and Hydroboration Applications. *Chem. Eur. J.* **23**, 16853-16861, (2017).
44 Jeong, E., Heo, J., Park, S. & Chang, S. Alkoxide-Promoted Selective Hydroboration of N-Heteroarenes: Pivotal Roles of in situ Generated BH3 in the Dearomatization Process. *Chem. Eur. J.* **25**, 6320-6325, (2019).
45 Kozuch, S. & Shaik, S. How to conceptualize catalytic cycles? The energetic span model. *Acc. Chem. Res.* **44**, 101-110, (2011).
46 Xu, P. & Xu, X. Dehydrogenation of (Di)amine–Boranes by Highly Active Scandocene Alkyl Catalysts. *Organometallics* **38**, 3212-3217, (2019).
47 Falivene, L. *et al.* Towards the online computer-aided design of catalytic pockets. *Nat. Chem.* **11**, 872-879, (2019).
48 Scerri, E. *The periodic table: its story and its significance*. (Oxford University Press, 2019).
49 Cheisson, T. & Schelter Eric, J. Rare earth elements: Mendeleev's bane, modern marvels. *Science* **363**, 489-493, (2019).

Acknowledgments: We thank the National Science Foundation grant CHE-1856619 (J.O.R., synthesis, characterization, catalysis), and the Office of Basic Energy Sciences, Department of Energy (DE-FG02-03ER154757) to the Institute for Catalysis in Energy Processes (ICEP) at Northwestern University (Y.K., T.J.M., experiment

design), for support of this research. This work made use of the IMSERC at Northwestern University, which has received support from the NSF (ECCS-2025633). Diffractometry experiments were conducted at IMSERC on Bruker Kappa APEX II instruments purchased with assistance from the State of Illinois and Northwestern University. Computational resources were provided by Northwestern University Quest High Performance Computing Cluster and CINECA award no. HP10CC5WSY 2020 under the ISCRA initiative. J.O.R. thanks Northwestern U. for an Academy Graduate Fellowship, Drs. Christopher Barger, Jiaqi Li, Tracy Lohr, and Victoria Weidner for helpful discussions, and Prof. Barbara Rothbaum, Dr. Alex Rothbaum, and Mr. John Rothbaum for edits.

Author contributions: J.O.R., Y.K., and T.J.M. conceived the idea and designed experiments. J.O.R. performed most experiments with aid from Y.K.. A.M. performed the DFT analysis. All authors analyzed the results and wrote the manuscript.

Competing interests: The authors declare no competing interests.

Additional information

Supplementary information is available for this paper

Correspondence and requests for materials should be addressed to A.M., Y.K., and T.J.M.

Reprints and permissions information is available at www.nature.com/reprints.

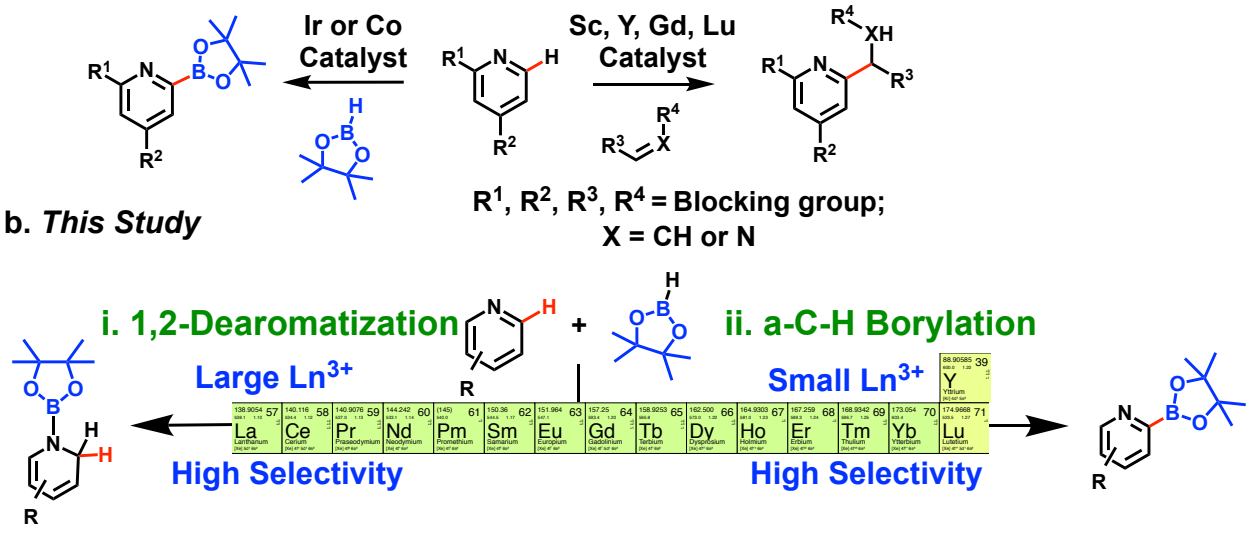

Figure 1. Recent progress towards α-borylated pyridinoid substrates via catalytic C-H functionalization. a. Early transition metal, lanthanide, and late transition metal catalyzed C-H functionalization and borylation of the pyridine α-positions **b.** This report of chemodivergent organolanthanide-catalyzed regioselective 1,2 –dearomatization or α-C-H functionalization of pyridine

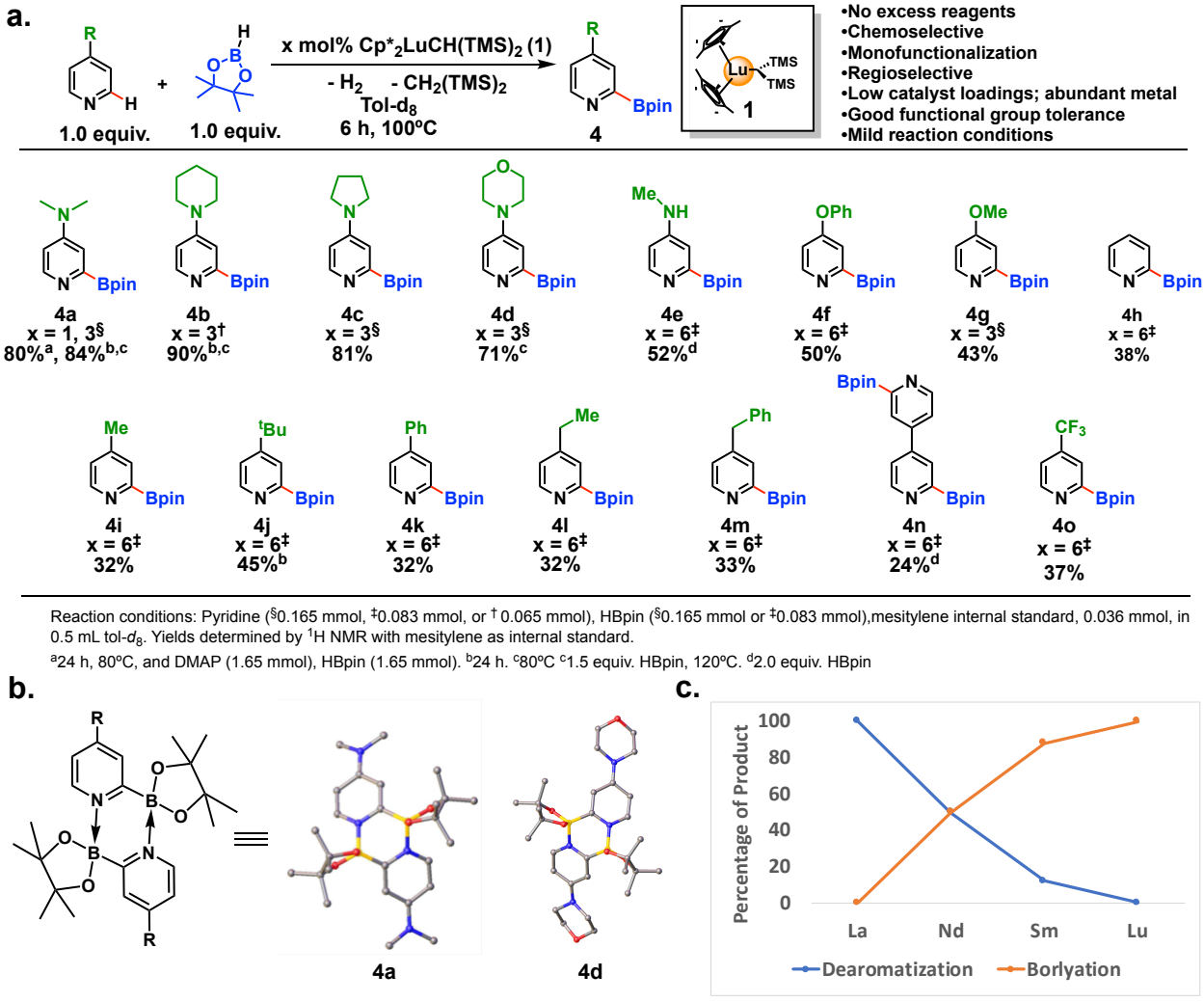

Figure 2. a. Substrate scope and yields for the Cp*$_2$Lu-catalyzed α-C-H borylation of variously substituted pyridines. **b.** Solid-state structures of products **4a** and **4d**. **c.** Experimental yields for 1,2–dearomatization (blue lines) vs C-H borylation (orange lines) for the indicated Cp$_2$*Ln- complexes.

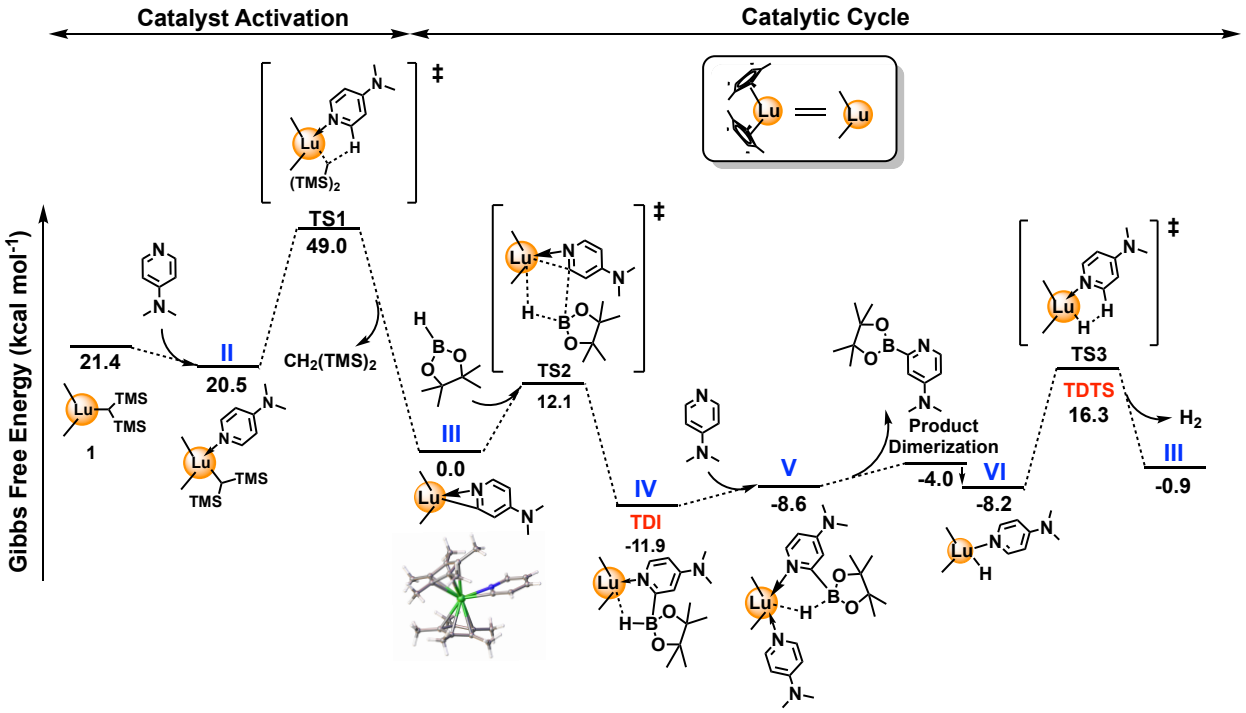

Figure 3. DFT-derived energetic profile for the C-H borylation of dimethylamino-pyridine (DMAP). Gibbs free energy profile (kcal mol^{-1}) associated with DMAP α-C-H borylation with HBpin mediated by precatalyst $Cp^*_2LuCH(TMS)_2$ and the diffraction-derived molecular structure of η^2-pyridine complex **III**.

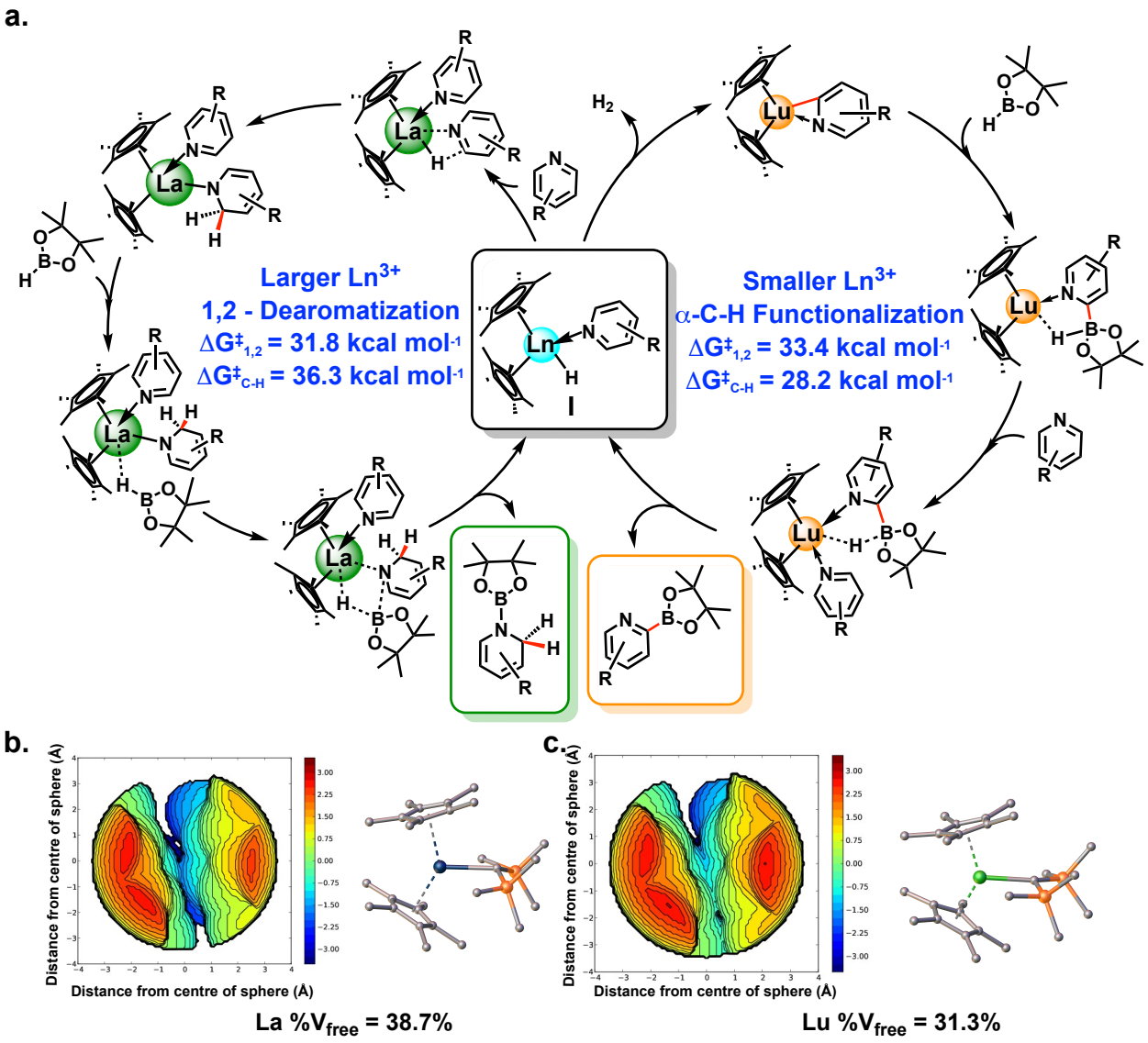

Figure 4. Mechanistic chemodivergence in pyridine HBpin functionalization mediated by Cp*$_2$Ln- catalysts as a function of Periodic Table location. **a.** Dual catalytic cycles for 1,2–dearomatization with Ln = La (left) vs C-H borylation with Ln = Lu (right). Key elements on the left side first proposed in ref. 40. X-ray crystal structures and computed percent free volume (%V_{free}) contours for Cp*$_2$LnCH(TMS)$_2$ complexes where Ln = **b.** La and **c.** Lu.